Electronic Supplementary Material (ESI) for Journal of Materials Chemistry C.


**Supplementary Information**

# Red thermally activated delayed fluorescence emitter employing dipyridophenazine with gradient multi-inductive effect to improve radiation efficiency

*Huiqin Wang,[a] Bingjie Zhao,[a] Peng Ma,[a] Zhe Li,[a] Xinyu Wang,[b] Chenxi Zhao,[a] Xiatao Fan,[a] Lilin Tao,[a] Chunbo Duan,[a] Jing Zhang,[a] Chunmiao Han,*[a] Guanying Chen,[b] and Hui Xu*[a]*

[a] Key Laboratory of Functional Inorganic Material Chemistry, Ministry of Education & School of Chemistry and Material Science, Heilongjiang University, Harbin, Heilongjiang 150080, China.

[b] School of Chemical Engineering and Technology, Harbin Institute of Technology, Harbin, Heilongjiang 150001, China.

## Content

# I. **Experimental Section**

## Materials and Instruments

All the reagents and solvents were purchased from Aldrich and Acros companies and used without further purification.

$^1$H NMR spectra were recorded using a Varian Mercury plus 400NB spectrometer relative to tetramethylsilane (TMS) as internal standard. Molecular masses were determined by a FINNIGAN LCQ Electro-Spraying Ionization-Mass Spectrometry (ESI-MS), or a MALDI-TOF-MS. Elemental analyses were performed on a Vario EL III elemental analyzer. Absorption and photoluminescence (PL) emission spectra of the target compound were measured using a SHIMADZU UV-3150 spectrophotometer and a SHIMADZU RF-5301PC spectrophotometer, respectively. Thermogravimetric analysis (TGA) and differential scanning calorimetry (DSC) were performed on Shimadzu DSC-60A and DTG-60A thermal analyzers under nitrogen atmosphere at a heating rate of 10 °C min$^{-1}$. Cyclic voltammetric (CV) studies were conducted using an Eco Chemie B. V. AUTOLAB potentiostat in a typical three-electrode cell with a platinum sheet working electrode, a platinum wire counter electrode, and a silver/silver nitrate (Ag/Ag$^+$) reference electrode. All electrochemical experiments were carried out under a nitrogen atmosphere at room temperature in dichloromethane. Phosphorescence spectra were measured in dichloromethane using an Edinburgh FPLS 920 fluorescence spectrophotometer at 77 K cooling by liquid nitrogen. The time decay spectra was measured using Time-Correlated Single Photon Counting (TCSPC) method with a microsecond pulsed Xenon light source for 1 μs-10 s lifetime measurement, the synchronization photomultiplier for signal collection and the Multi-Channel Scaling Mode of the PCS900 fast counter PC plug-in card for data processing.

## Synthetic procedure

The ***o*TPA-DPPZ** and intermediates were fully characterized by $^1$H NMR, MALDI-TOF, element analysis and single crystal X-ray diffraction analysis.

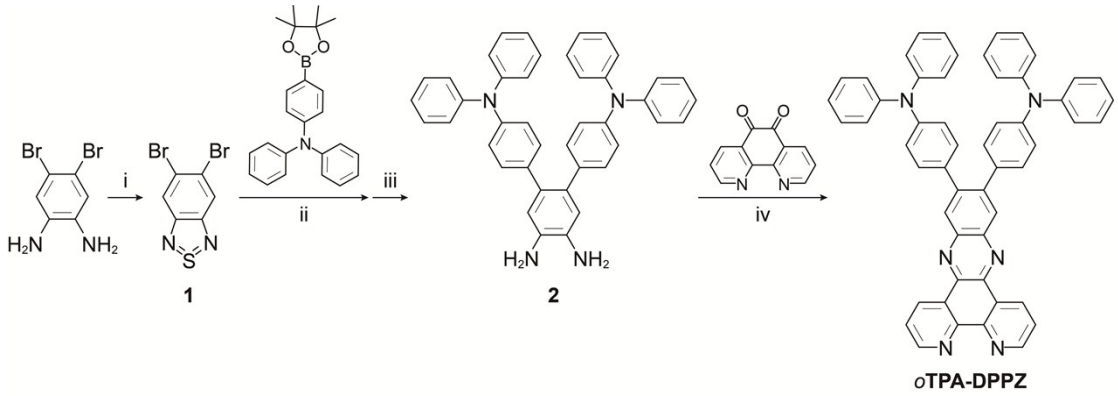


**Scheme S1.** Synthetic procedure of ***o*TPA-DPPZ**: i. $SOCl_2$, $Et_3N$, $CH_2Cl_2$, 45 °C, 5 h; ii. $Pd(PPh_3)_4$, TBAB, toluene, 100 °C, 24 h; iii. $NaBH_4$, $CoCl_2$, $CH_3OH/CH_2Cl_2$, 0.5 h; iv. $CH_2Cl_2$, 60 °C, 8 h

**5,6-dibromobenzo[c][1,2,5]thiadiazole (1)**

5.32 g of 4,5-dibromobenzene-1,2-diamine (0.02 mol) and 12 mL of $Et_3N$ (0.08 mol) were dissolved in 60 mL of dry $CH_2Cl_2$ at 0 °C. A solution of thionyl chloride (0.05 mol, 3.80 mL) in 10 mL of $CH_2Cl_2$ was added to the mixture, and stirred for 5 h under reflux. After cooling to room temperature, the mixture was filtered and the solvent was removed in *vacuum*. The residue was purified with column chromatography. Yield: 90%. $^1$H NMR (TMS, $CDCl_3$, 400 MHz): $\delta$ = 9.39 (s, 2H). LDI-TOF: m/z (%): 293 (100) [$M^+$].

**$N^4$,$N^4$,$N^{4''}$,$N^{4''}$-tetraphenyl-[1,1':2',1''-terphenyl]-4,4',4'',5'-tetraamine (2)**

In $Ar_2$, 12 mmol of aq. NaOH (2M) was added to a stirred solution of **1** (1 mmol, 0.2940 g), N,N-diphenyl-4-(4,4,5,5-tetramethyl-1,3,2-dioxaborolan-2-yl)aniline (1 mmol, 0.3712 g), TBAB (0.2 mmol, 0.064 g) and $Pd(PPh_3)_4$ (0.025 mmol, 0.0289 g) in 20 mL of toluene. The mixture was heated to 110 °C and stirred for 24 h. The reaction was quenched by aq. $NH_4Cl$, and extracted with $CH_2Cl_2$. The organic layer was dried with anhydrous $Na_2SO_4$. The solvent was removed in *vacuo*. The crude was dissolved in $CH_2Cl_2$ (100 mL). 50 mL of methanol was added and stirred for 30 min. $CoCl_2 \cdot 6H_2O$ (1 mmol, 0.1189 g), methanol (60 mL) and $NaBH_4$ (5 mmol, 0.1861 g) were added to the reaction mixture and stirred for 30 min. The reaction was quenched with water and extracted with $CH_2Cl_2$. The organic layer was dried with anhydrous $Na_2SO_4$. The solvent was removed in *vacuo*. The crude was purified by column

chromatography. Yield: 80%. $^1$H NMR (TMS, $CDCl_3$, 400 MHz): $\delta$ =7.20 (t, $J$ = 8 Hz, 8H), 7.05 (d, $J$ = 8 Hz , 8H), 6.97 (t, $J$ = 8 Hz ,8H), 6.92 (d, 8 $J$ = 12 Hz ,4H), 6.7 (s, 2H ), 3.39 (s, 4H). LDI-TOF: m/z (%): 594 (100) [$M^+$]; elemental analysis (%) for $C_{42}H_{34}N_4$: C 84.82; H, 5.76; N, 9.42; found: C 84.72; H, 5.78; N, 9.47.

**4,4'-(9a,13a-dihydrodipyrido[3,2-a:2',3'-c]phenazine-11,12-diyl)bis(N,N-diphenylaniline) (*o*TPA-DPPZ)**

A mixture of **2** (5 mmol, 2.971 g), 1,10-phenanthroline-5,6-dione (5 mmol, 1.05 g) and $CH_2Cl_2$ (50 mL) were heated to 60 °C and stirred for 8 h. The reaction was quenched with water and extracted with $CH_2Cl_2$. The organic layer was dried with anhydrous $Na_2SO_4$. The solvent was removed in *vacuo*. The crude was purified by column chromatography. Yield: 90%. $^1$H NMR (TMS, $CDCl_3$, 400 MHz): $\delta$ = 9.65 (dd, $J_1$= 1.6 Hz, $J_2$= 8.0 Hz, 2H), 9.27 (dd, $J_1$= 1.6 Hz, $J_2$ = 4.4 Hz, 2H ), 8.39 (s, 2H), 7.90 (dd, $J_1$ = 4.4 Hz, $J_2$ = 8.0 Hz, 2H), 7.28 (m, 8H), 7.22 (d, $J$ = 8.4 Hz, 4H), 7.14 (d, $J$ = 7.6 Hz, 8H), 7.06 (t, $J$ = 7.4 Hz, 8H). LDI-TOF: m/z (%): 768 (100) [$M^+$]; elemental analysis (%) for $C_{54}H_{36}N_6$: C, 84.35; H, 4.72; N, 10.93; found: C, 84.40; H, 4.73; N, 10.90.

CIF file of ***o*TPA-DPPZ** can also be obtained free of charge from the Cambridge Crystallographic Data Centre, under deposition number CCDC 1910979.

**DFT Calculations**

DFT computations were carried out with different parameters for structure optimizations and vibration analyses. The ground states of molecules in *vacuum* were optimized without any assistance of experimental data by the restricted and unrestricted formalism of Beck's three-parameter hybrid exchange functional[1] and Lee, and Yang and Parr correlation functional[2] (B3LYP) for C, H, N, and O. The optimization was performed at the level of 6-31G(d). The fully optimized stationary points were further characterized by harmonic vibrational frequency analysis to ensure that real local minima had been found without imaginary vibrational frequency. The total energies were also corrected by zero-point energy both for the ground state. All computations were performed using the Gaussian 03 package.[3]

**Experimental Oscillator Strength Calculation**

The experimental oscillator strength (*f*) was calculated from the absorption spectra using the following equa.[4-7]

$$f = 4.31 \times 10^{-9} \int \varepsilon dv$$

Where ε is the molar extinction coefficient, υ is the absorption wavenumber.

**Device Fabrication and Testing**

Before loading into a deposition chamber, the ITO substrate was cleaned with detergents and deionized water, dried in an oven at 120 °C for 4 h, and treated with UV-ozone for 20 min. Devices were fabricated by evaporating organic layers at a rate of 0.1-0.3 nm $s^{-1}$ onto the ITO substrate sequentially at a pressure below $1\times10^{-6}$ mbar. Onto the electron transporting layer, a layer of LiF with 1 nm thickness was deposited at a rate of 0.1 nm $s^{-1}$ to improve electron injection. Finally, a 100-nm-thick layer of Al was deposited at a rate of 0.6 nm $s^{-1}$ as the cathode. The emission area of the devices was 0.09 $cm^2$ as determined by the overlap area of the anode and the cathode. The EL spectra and CIE coordinates were measured using a PR655 spectra colorimeter. The current-density-voltage and brightness-voltage curves of the devices were measured using a Keithley 4200 source meter and a calibrated silicon photodiode. All the measurements were carried out at room temperature in glove box. For each emitter, four devices were fabricated in parallel to confirm the performance repeatability

## II. Thermal property

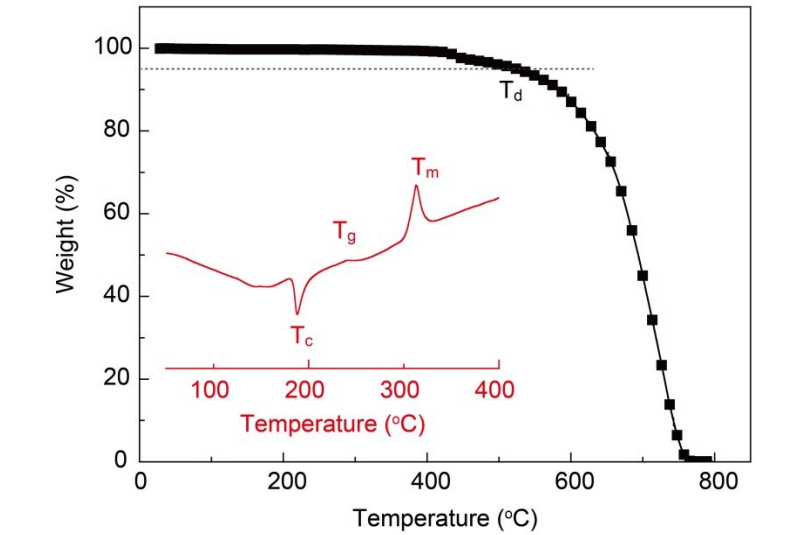


**Figure S1.** TGA and DSC (inset) curves of ***o*TPA-DPPZ**.

## III. DFT simulation results

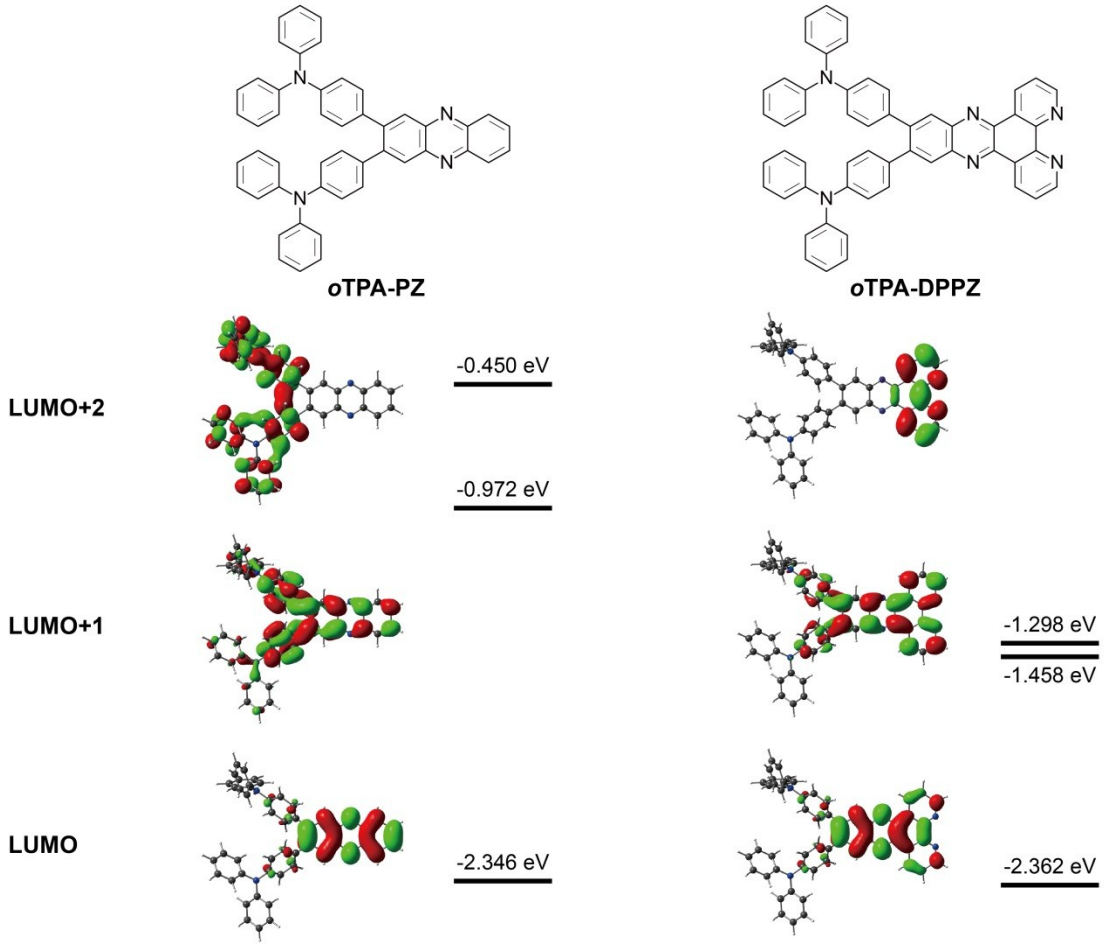


**Figure S2.** Contours and energy levels of the first three unoccupied (LUMO~LUMO+2) molecular orbitals for ***o*TPA-PZ** and ***o*TPA-DPPZ** simulated with the DFT method.

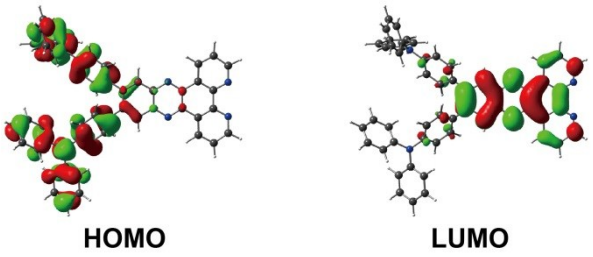


**Figure S3.** Contours of the HOMO and LUMO of ***o*TPA-DPPZ** simulated with the DFT method.

# IV. Single crystal X-ray diffraction result

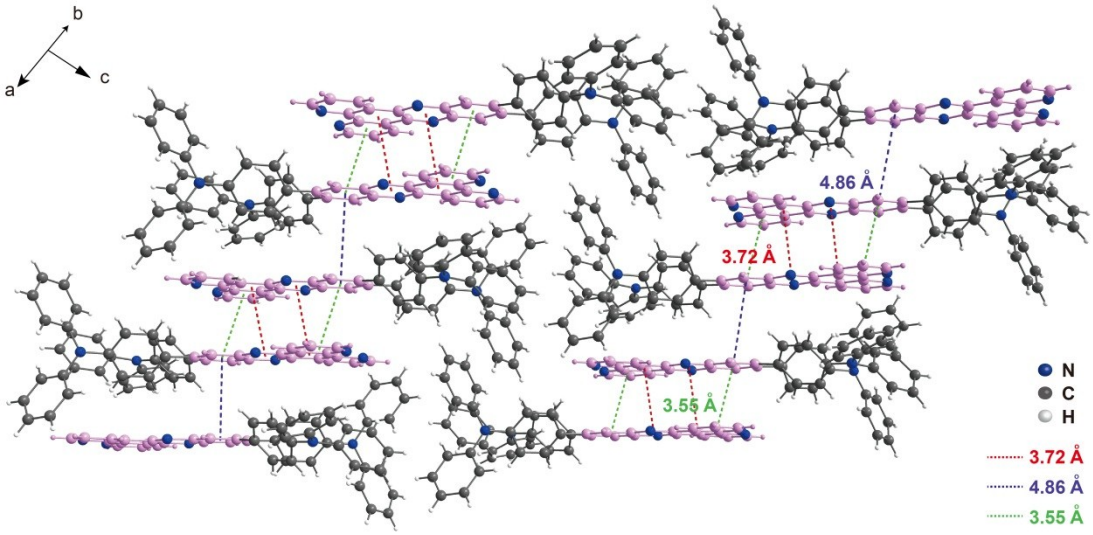


**Figure S4.** Single crystal packing diagram of ***o*TPA-DPPZ**.

## V. Photophysical properties

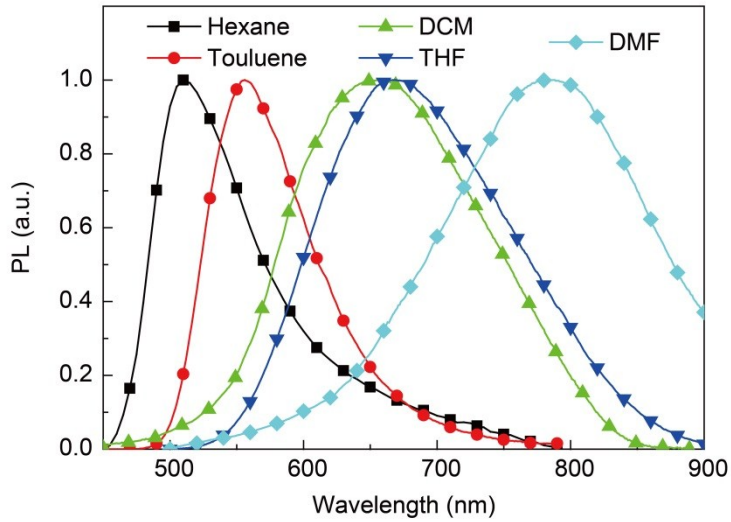


**Figure S5.** PL spectra of ***o*TPA-DPPZ** in different solvents. DCM, THF and DMF are dichloromethane, tetrahydrofuran and dimethylformamide, respectively.

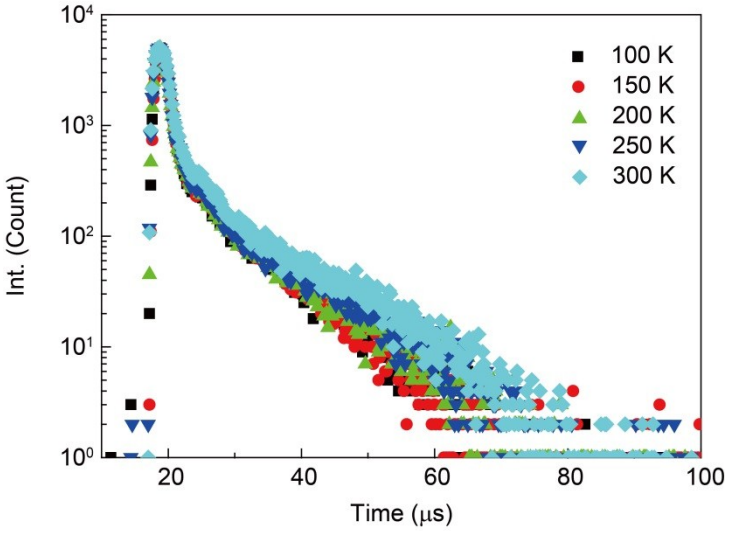


**Figure S6.** Time decay curves of ***o*TPA-DPPZ** in DCM at temperature ranging from 100 K to 300 K.

**Table S1. Physical properties of *o*TPA-DPPZ**

| Absorption (nm) | PL (nm) | PLQY[c] (%) | $S_1/T_1$ (eV) | $T_g/T_m/T_d$ (°C) | HOMO/LUMO (eV) |
|---|---|---|---|---|---|
| 280, 329,458[a] | 654[a] | 33.77[a] | 2.37/2.29[d] | 242/312/524 | -5.002/-2.362[e] |
| 287,342,483[b] | 625[b] | 27.34[b] | 2.31/2.10[e] | | -5.779/-3.768[f] |

[a]In DCM ($10^{-5}$ mol $L^{-1}$); [b]in solid film; [c]Absolute PL quantum yield evaluated using an integrating sphere; [d]Estimated according to the 0-0 transition of fluorescence and phosphorescence spectra, respectively; [e]TD-DFT calculated results; [f]Calculated according the onset voltages of redox peaks with the equation of -($V_{onset}$ + 4.78) eV.

**Table S2. Photophysical parameters of 30% *o*TPA-DPPZ doped DBFDPO film**

| PL (nm) | $\eta$[a] (%) | $\tau$[b] (ns) | $\tau$[c] ($\mu$s) | $\eta_{PF}$[d] (%) | $\eta_{DF}$[e] (%) | $k_{PF}$[f] ($10^7$ $s^{-1}$) | $k_{DF}$[g] ($10^5$ $s^{-1}$) | $k_{RISC}$[h] ($10^4$ $s^{-1}$) | $k_{rS}$[i] ($10^6$ $s^{-1}$) |
|---|---|---|---|---|---|---|---|---|---|
| 605 | 75 | 22 | 17 | 25.5 | 49.5 | 1.2 | 0.3 | 0.9 | 3.0 |

[a]Absolute PLQY evaluated using an integrating sphere; [b,c]prompted and delayed emission lifetime; [d,e]PLQY of prompted and delayed emissions estimated according to the corresponding proportions in transient decay curves; [f,g]Rate constants of prompted and delayed emission; [h]Rate constants of reverse intersystem crossing; [i]Rate constants of singlet radiation.

## VI. Electrochemical property

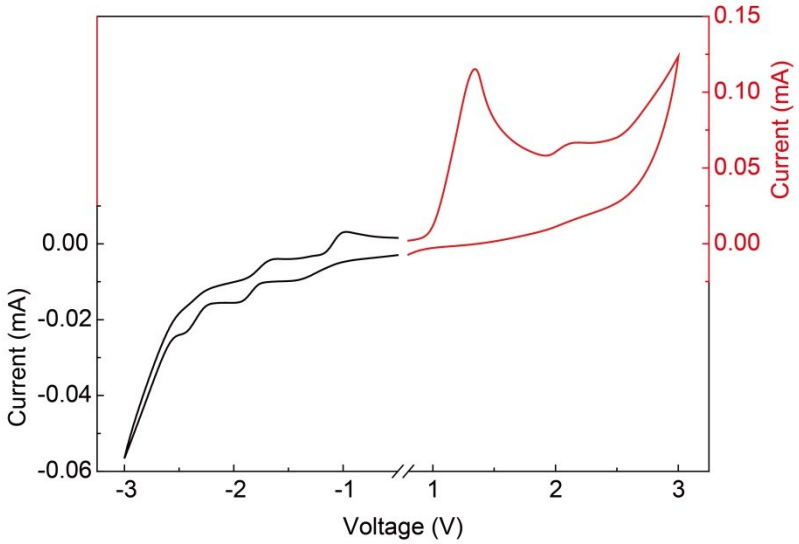


**Figure S7.** Cyclic voltammogram of ***o*TPA-DPPZ** measured in DCM for oxidation and THF for reduction at room temperature with the scanning rate of 100 mV $S^{-1}$ and tetra-*n*-butylammonium hexafulorophosphate as supporting electrolyte (0.1 mol $L^{-1}$).

## VII. Carrier transporting ability

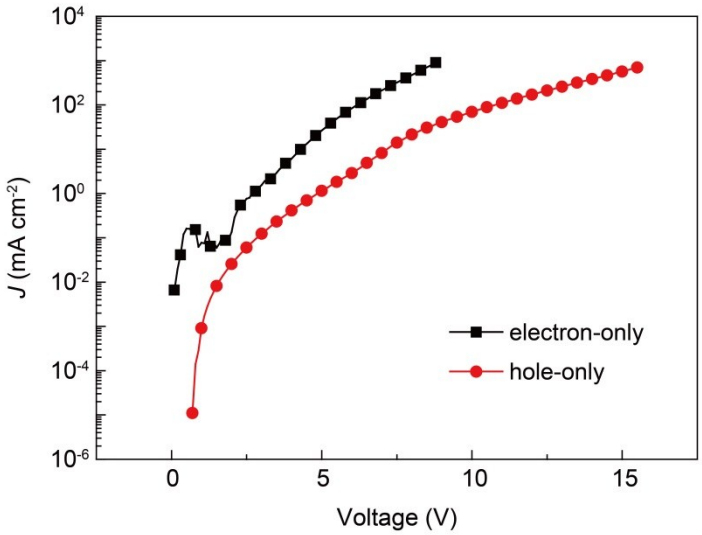


**Figure S8.** Current density (*J*)-voltage relationship of single-carrier transporting devices with configurations of ITO|LiF (1 nm)|***o*TPA-DPPZ** (100 nm)|LiF (1 nm)|Al (100 nm) for electron-only and ITO|$MoO_3$ (6 nm)|***o*TPA-DPPZ** (100 nm)| $MoO_3$ (6 nm)|Al (100 nm) for hole-only, respectively.

## VIII. Electroluminescence performance

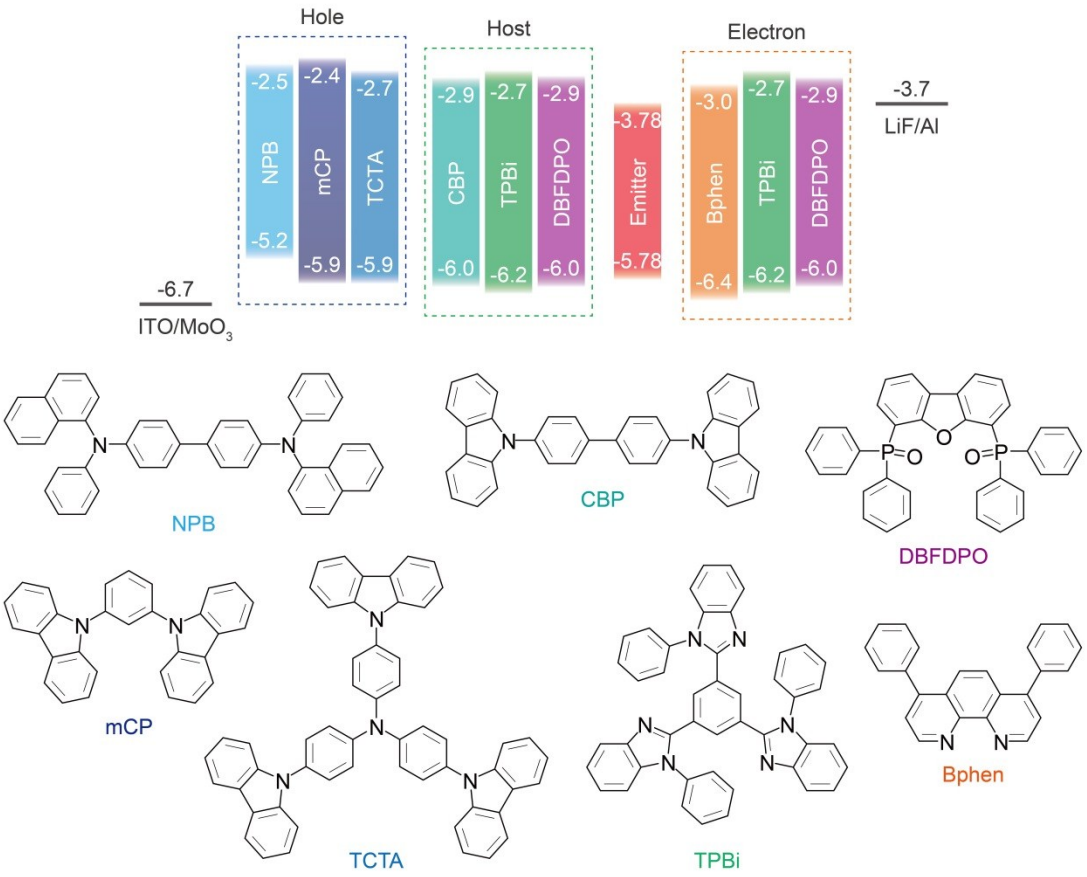


**Scheme S2.** Energy level of devices based on ***o*TPA-DPPZ** and the chemical structures of the involved materials.

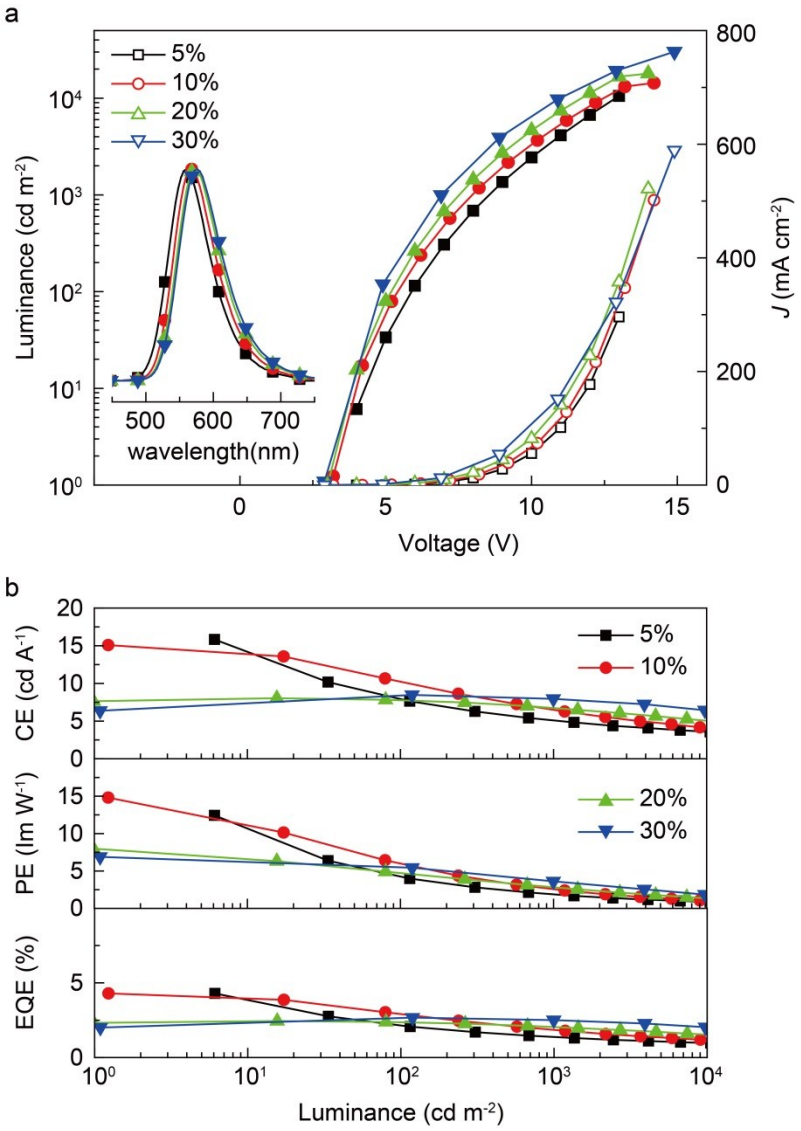


**Figure S9.** (a) Luminance-*J*-Voltage curves and EL spectra (inset) of ***o*TPA-DPPZ** based device using CBP as host, with ***o*TPA-DPPZ** doping concentrations of 5, 10, 20 and 30%, respectively; (b) Efficiency *vs.* Luminance curves of the devices.

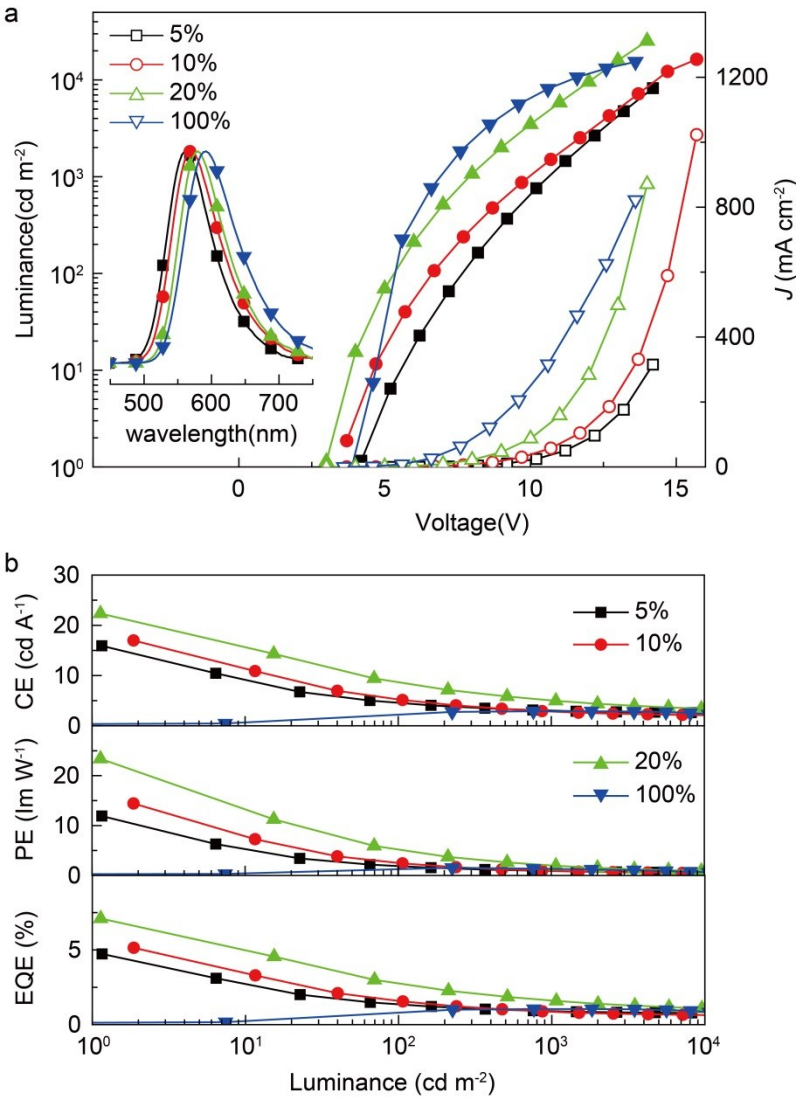


**Figure S10.** (a) Luminance-*J*-Voltage curves and EL spectra (inset) of ***o*TPA-DPPZ** based device using TPBi as host, with ***o*TPA-DPPZ** doping concentrations of 5, 10, 20 and 100%, respectively; (b) Efficiency *vs.* Luminance curves of the device.

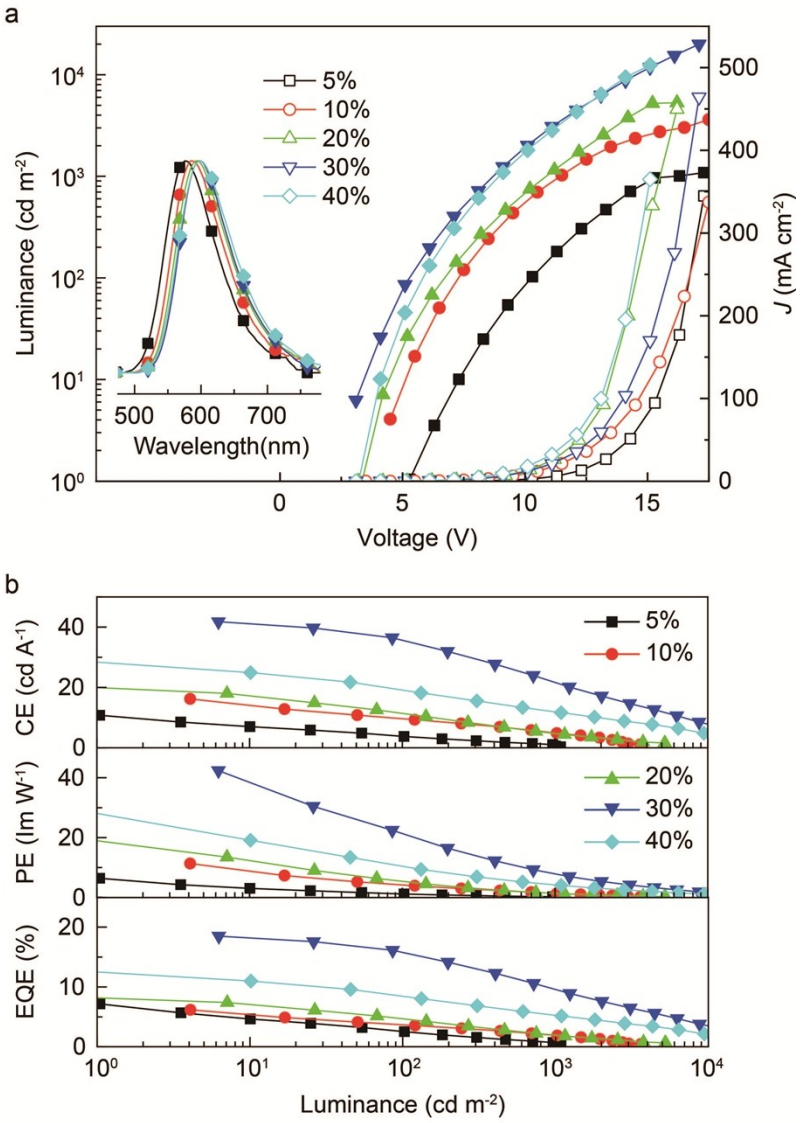


**Figure S11.** (a) Luminance-*J*-Voltage curves and EL spectra (inset) of ***o*TPA-DPPZ** based device using DBFDPO as host, with ***o*TPA-DPPZ** doping concentrations of 5, 10, 20, 30 and 40%, respectively; (b) Efficiency *vs.* Luminance curves of the devices.

## IX. References


[1] A. D. Becke, *J. Chem. Phys.* **1993**, *98*, 5648-5652.

[2] C. Lee, W. Yang and R. G. Parr, *Phys. Rev. B* **1988**, *37*, 785-789.

[3] M. J. Frisch, G. W. Trucks, H. B. Schlegel, G. E. Scuseria, M. A. Robb, J. R. Cheeseman, J. A. Montgomery, J. T. Vreyen, K. N. Kudin, J. C. Burant, J. M. Millam, S. S. Iyengar, J. Tomasi, V. Barone, B. Mennucci, M. Cossi, G. Scalmani, N. Rega, G. A. Petersson, H. Nakatsuji, M. Hada, M. Ehara, K. Toyota, R. Fukuda, J. Hasegawa, M. Ishida, T. Nakajima, Y. Honda, O. Kitao, H. Nakai, M. Klene, X. Li, J. E. Knox, H. P. Hratchian, J. B. Cross, C. Adamo, J. Jaramillo, R. Gomperts, R. E. Stratmann, O. Yazyev, A. J. Austin, R. Cammi, C. Pomelli, J. W. Ochterski, P. Y. Ayala, K. Morokuma, G. A. Voth, P. Salvador, J. J. Dannenberg, V. G. Zakrzewski, S. Dapprich, A. D. Daniels, M. C. Strain, O. Farkas, D. K. Malick, A. D. Rabuck, K. Raghavachari, J. B. Foresman, J. V. Ortiz, Q. Cui, A. G. Baboul, S. Clifford, J. Cioslowski, B. B. Stefanov, A. L. G. Liu, P. Piskorz, I. Komaromi, R. L.Martin, D. J. Fox, T. Keith, M. A. Al-Laham, C. Y. Peng, A. Nanayakkara, M. Challacombe, P. M. W. Gill, B. Johnson, W. Chen, M. W. Wong, C. Gonzalez and J. A. Pople, *Gaussian 03, Revision D.02, Gaussian Inc., Pittsburgh, PA* **2004**.

[4] A. Maccoll, *Quart. Rev.,* **1947**, *1*, 16-58.

[5] V. J. Hammond, W. C. Price, *Trans. Faraday Soc.,* **1955**, *51*, 605-610.

[6] J. Ferguson, L. W. Reeves, W. G. Schneider, *Can. J. Chem.*, **1957**, *35*, 1117-1136.

[7] Turro, N. J.; Ramamurthy, V.; Scaiano, J. C. *Modern Molecular Photochemistry of Organic Molecules*; University Science Books: Sausalito, CA, **2010**.